Int. J. Electrochem. Sci., 10 **(2015)** 6794 - 6802

International Journal of
ELECTROCHEMICAL
SCIENCE
www.electrochemsci.org

Short Communication

Preparation of Graphene Aerogel for Determining Oxalic Acid

Dandan Liu[*], *Yaoxian Wang and Ganqing Zhao*

Key laboratory of ecological restoration in hilly area, Pingdingshan University, Pingdingshan, P. R. China
[*]E-mail: dandanliu652@yahoo.com

Received: 25 April 2015 / *Accepted:* 27 May 2015 / *Published:* 24 June 2015

In this paper, we developed an electrochemical sensor for the detection of oxalic acid (OA). The electrochemical sensor was prepared by hydrothermal synthesis of three dimensional (3D) graphene aerogel (GA). The obtained sensor was characterized by a series of techniques. It was found that the GA modified GCE displays excellent catalytic property toward the oxidation of OA, which make it became an enzymeless sensor with high selectivity, good reproducibility and stability. The sensor shows a linear relation towards OA detection in the concentration of 4 to 100 μM with a low detection limit of 0.8 μM. Moreover, the proposed sensor was used for OA detection in tomato and onion samples.

Keywords: Graphene aerogel; oxalic acid; Electrochemical sensor; Tomato; Onion

1. INTRODUCTION

Oxalic acid (OA) is a kind of calcium and magnesium salts present in plant cells and cell walls [1]. In human, precipitation of calcium oxalate could lead to the formation of kidney stones [2]. Therefore, the detection of OA is considerable important, especially for clinical diagnosis. To date, many techniques have been developed for the detection of OA such as gas chromatography [3], liquid chromatography [4], flow-injection catalytic spectrophotometry [5], ion exclusion chromatography and enzymatic methods [6, 7]. Among these approaches, due to the relatively high efficiency, cost-effectiveness, speed, portability, ease of operation and reliability, electrochemical methods have become an important investigation domain for OA detection [8-11].

Different materials have been introduced into the electrochemical biosensor to improve its detection sensitivity. For example. platinum, gold, palladium and boron-doped diamond electrode has been extensively studied [12-15]. Nevertheless, the oxidation of OA at normal electrodes commonly

needs high overpotential. Therefore, different methods were developed for electrode surface modification such as cobalt phthalocyanine chemically modified glassy carbon (GC) electrode, Rh octaethylporphyrin modified carbon black electrode, SiO_2/SnO_2 mixed oxide, carbon nanotubes modified GC electrode, Pd NPs loaded carbon nanofiber modified carbon paste electrode and exfoliated graphite-polystyrene composite electrode have been developed to study the electrocatalytic oxidation of OA [16-22].

Herein, we proposed a method for fabrication of an OA electrochemical sensor based on graphene aerogel modified electrode. The synthesized hybrid thin film was characterized by SEM, Raman spectroscopy and XRD. The fabricated sensor was used for OA detection by cyclic voltammetry. The result exhibited that the oxidation of OA was significantly enhanced by the graphene aerogel. With such a graphene aerogel modified electrode, OA in tomato and onion was successfully detected.

2. EXPERIMENTS

Synthetic graphite, potassium permanganate was purchased from Tianjin Jiangtian Chemical Reagent Co. Oxalic acid was purchased from Sigma-Aldrich. All other chemicals were analytical grade.

Graphene oxide (GO) was fabricated based on the modified Hammer's method [23, 24]. To synthesize the self-assembled three dimensional reduced GO, 40 mL solution of 1 mg/mL homogeneous GO aqueous dispersion was sonicated for 15 minutes and then transfer to a 25-mL Teflon-lined autoclave for hydrothermal reaction at 180 °C for 18 hours. Then the autoclave left outside to cool naturally at room temperature and then the reduced graphene oxide hydrogel were taken out with help of tweezers and put on filter paper in order remove surface adsorbed water. Then for characterization purposes samples were transferred to freezer for 48 hours and then freeze-drying for 24 h, freeze drying is used to fix three dimensional structure made by interlinked G-sheets and yields spongy assembly, after this all the solvents in as prepared hydrogel is removed and final 3D graphene aerogels were synthesized that retain the morphology of parent hydrogel.

The morphology of the GA was characterized using a scanning electron microscope (SEM, S-4700, Hitachi). Raman spectra of samples were collected at a Raman Microprobe (Renishaw RM1000) with 514 nm laser light. The crystal information of samples were characterized from 5° to 80° in 2θ by a XRD (D8-Advanced, Bruker). The surface functional groups present on the samples were characterized by a Fourier transform infrared spectroscopy (FTIR, Nicolet iS5, Thermo Scientific, USA).

A glassy carbon electrode (GCE) was polished with alumina-water slurry followed by washing process. For the GCE surface modification, 5 μL of PDA-RGO/Ag composite dispersion (1 mg/mL) was carefully dropped onto the GCE and dried at a fume hood. The cleaned GCE was coated by casting 5 μL of the black graphene aerosol suspension and dried at a fume hood as well. Electrochemical measurements were performed on a CHI430A electrochemical workstation, by a three-electrode system. A platinum electrode was used as the auxiliary electrode and an Ag/AgCl (3M

KCl) as the reference electrode. All electrochemical measurements were carried out in a pH 7.0 PBS at the room temperature.

3. RESULTS AND DISCUSSION

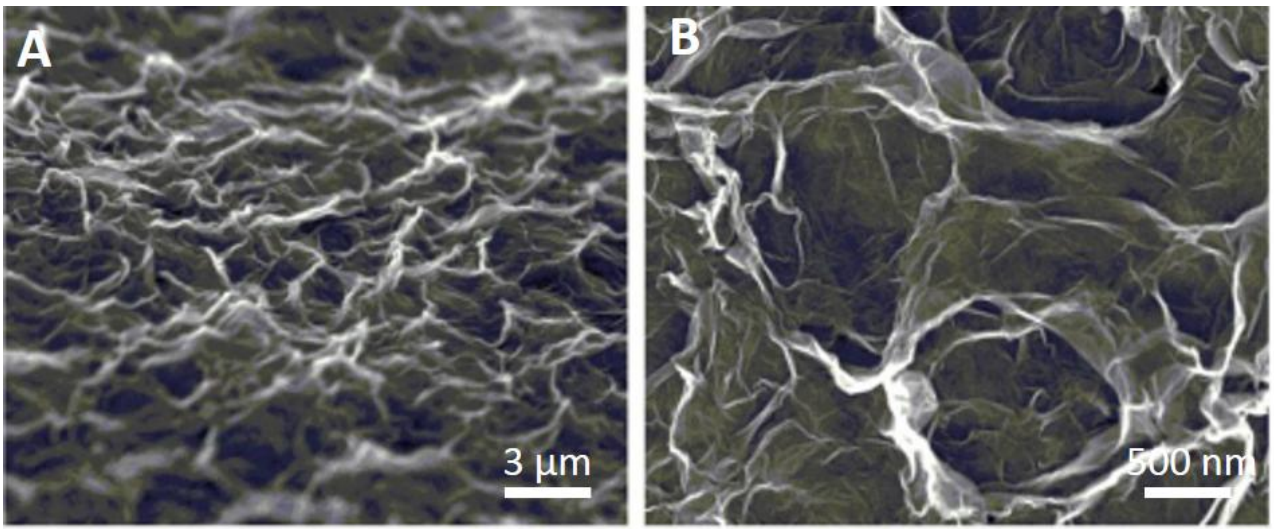

Figure 1. SEM images of GA at (A) low magnification and (B) high magnification.

The morphology of the prepared thin films was characterized by SEM. Figure 1 displays the SEM images of GA at different magnifications. It can be observed that the GA shows interconnected porous structure. The porosity of GO aerogels can be adjusted by changing the concentration of the GO in the preparing procedure. They are randomly distributed over the aerogel and have a regular arrangement. This porous network structure could provide a large specific surface area, which is favorable for the electrochemical reaction. The XRD patterns of GO and GA are presented in Figure 2. It can be seen that the pristine GO displays a typical characteristic (001) peak at 11.1°. From brags equation, the interlayer spacing of GO is estimated around 9 Å which is due to the oxygen functional groups in GO and definitely much higher than interlayer spacing in graphite at (002) diffraction peak reflection (about 3 Å). This increment is due to oxygen-containing functional groups presence on GO sheets. The sharp peak $2\theta=10°$ of GA disappeared at diffraction pattern, which bring more evidence for the reduction of GO. So the interlayer spacing of the GA is estimated around 3.83 Å. These results indicate the presence of some oxygenated functional groups on GA sheets and they can help for water encapsulation during self-assembly due to their hydrophilic properties. In addition, this restacking of graphene sheets led to effective preparation of reduced graphene oxide hydrogel. Finally broad peak of XRD pattern of GA implies poor crystalline of graphene sheets along the stacking direction and demonstrate that the structure of the GA is consist of stacking of few layers graphene sheets.

The electro-reduction process and bonding interactions between ZnO and RGO was investigated by FTIR study.

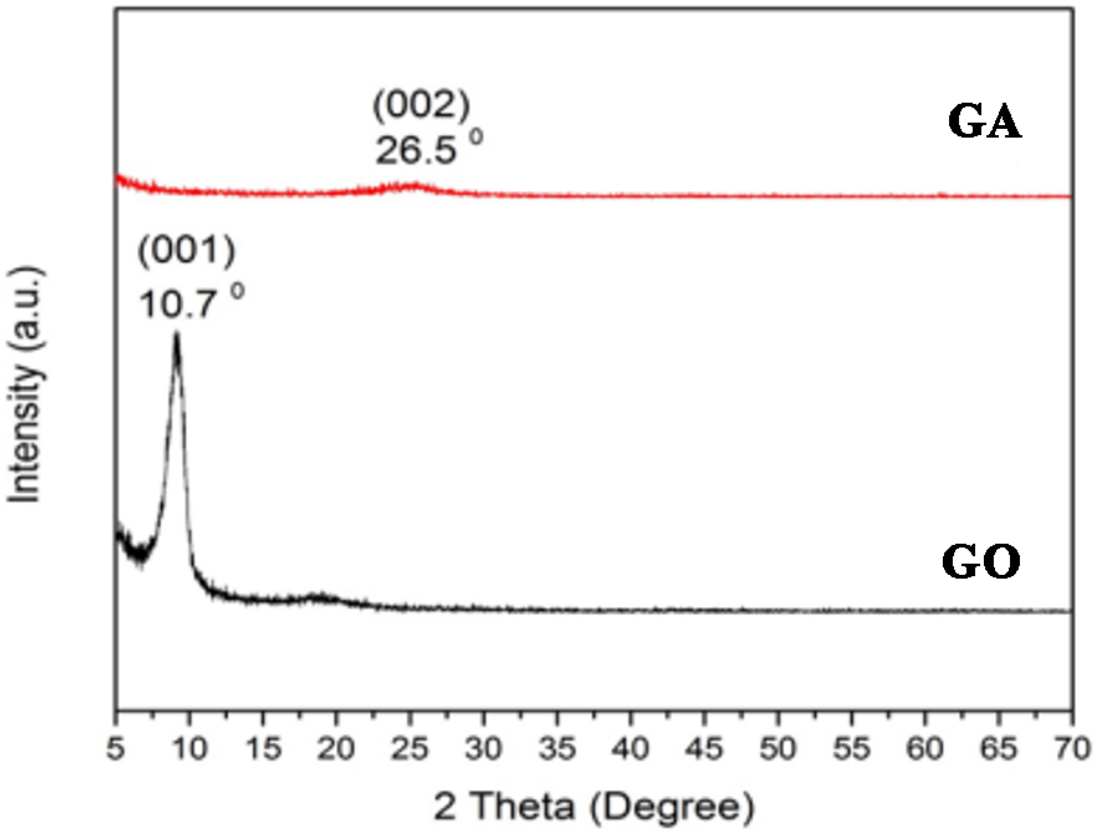

Figure 2. XRD spectra of GO and synthesized GA.

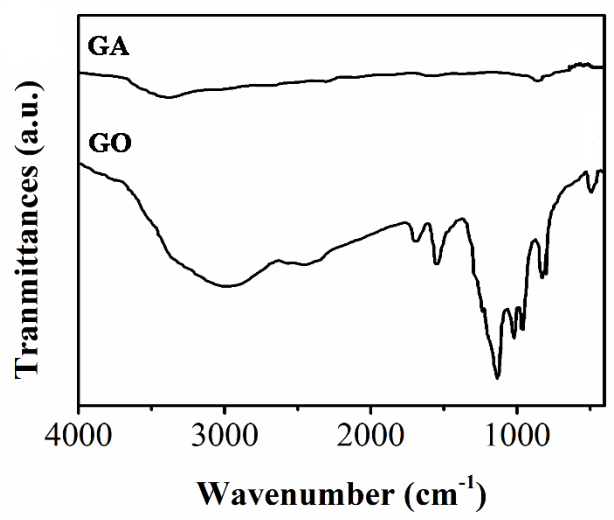

Figure 3. FTIR spectra of GO and GA.

Figure 3 displays the FTIR spectra of GO and GA. The spectrum of GO shows peaks at 2940 cm^{-1}, 1729 cm^{-1}, 1401 cm^{-1} and 1052 cm^{-1}, which belong to the vibration of CH_2, C═O stretching of COOH groups, C─OH vibrations and C─O vibrations from alkoxy groups, respectively [25, 26]. The

broad peak at 3342 cm^{-1} is assigned to the OH stretching vibration of oxygen functional groups. In addition, the peak at 1619 cm^{-1} is due to the sp^2 bond of graphite in GO [27]. Comparing spectra of GA with the GO, it is noticeable that the peaks related to oxygen functional groups are almost removed in GO by electro-reduction process, indicating the GO has been reduced considerably.[28]

To further evaluate the degree of the sp^2 network during the hydrothermal process, Raman spectroscopy of GO and GA was carry out (not shown). Two broad peaks are well known for materials, G mode due to first order scattering of the E_{2g} photon of sp^2 C atoms (~1585 cm^{-1}), and D mode due to the breathing mode of j-point photons of A_{1g} symmetry (~1348 cm^{-1}). GA shows higher intensity ratio of D-band to G-band, which indicating the increasing of the number of smaller graphene domains [29, 30].

The electrocatalytic property of graphene aerosol film modified GCE (GA/GCE) towards OA electrooxidation in buffer solution (pH 7.00) was measured by cyclic voltammetry (CV). As shown in Figure 3, the higher oxidation response is obtained with lower potential for OA at GA/GCE. In contrast, pure GCE displays an oxidation wave at 1.4 V for OA (curve c). Moreover, the GA/GCE displays a well-defined oxidation peak for OA at 1.15 (curve d). The obtained CV signal with higher oxidation current and less positive potential for OA at GA/GCE is attributed by the excellent electrocatalytic property of graphene aerosol.

Also, the CVs of the GA/GCE in 0.1 M PBS (pH 7.00) in presence of 0.03 mM OA at various scan rates were investigated. It can be seen that the anodic peak current is linearly proportional to square scan rate, indicating that the oxidation of OA at electrode surface is controlled by diffusion.

It well known, the pH value of electrolyte could affect the electrochemical behavior of OA at electrode surface. The effect of pH value on the electro-oxidation of OA at the GA/GCE was investigated at pH range between 3.00 to 9.00. The results show that the current response of OA at GA/GCE gradually increases from pH 3.00 to 7.00 and then decreasing (not shown). Therefore, pH 7.00 was chosen as optimum pH condition.

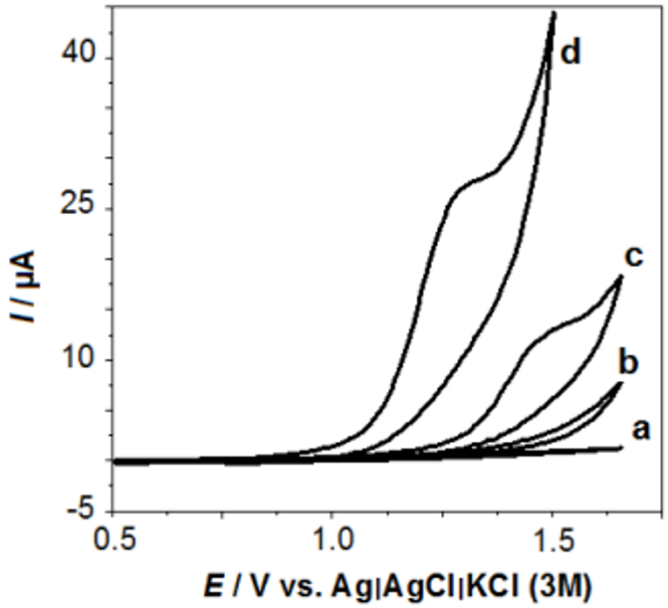

Figure 4. CVs of (a) GCE and (b) GA/GCE in absence of OA and (c) GCE and (d) GA/GCE in presence of 0.01 mM in 0.1 M PBS (pH 7.00) at scan rate 50 mV/s.

Figurea 4 shows the cyclic voltammograms obtained for OA at GA/GCE in 0.1 M PBS. It can be seen that the oxidation current of OA at GA/GCE surface has a linear relationship with OA concentration at range of 4–100 μM. The detection limit can be calculated as 0.8 μM. The sensitivity can be calculated as 677.98 μA mM−1 with a correlation coefficient of 0.9901 (Figure 4, inset).

Table 1. Comparison of OA detection using our proposed method with other literatures.

Electrode	LDR[a] (μM)	LOD[b] (μM)	Sensitivity (Ma/mM)	Reference
EF-PS[c]	500-3000	50	0.6	[31]
TiO_2/MWCNTs/GC[d]	100-1000	33	-	[32]
Pd/CNF/CP[e]	20-13000	20	-	[20]
BDD[f]	0.05-10	0.0005	-	[33]
GA/GCE	4-100	0.8	677.98	This work

[a] Linear Dynamic Range
[b] Limit of Detection
[c] Exfoliated Graphite-Polystyrene
[d] TiO_2 nanoparticles/multi walled carbon nanotubes/Glassy Carbon
[e] Palladium nanoparticle-loaded carbon Nano Fiber/Carbon Paste
[f] Boron-Doped Diamond

The observed linear range and detection limit of OA were compared with the reported papers and are given in Table 1. As can be seen from Table 1, analytical parameters for OA detection of the sensor prepared in this work are comparable with other results. It can be conclude that, our proposed OA sensor was highly stable and no tedious procedure was involved in electrode modification.

The reliability of the proposed OA sensor was tested. The GA/GCE was applied to analysis of OA in onion and tomato samples by cyclic voltammetry measurement. 1 mL of the onion and tomato water samples was diluted to 10 mL of 0.1 M PBS. The standard addition technique was used to investigated the recovery of OA in onion and tomato samples. The analytical results are summarized in Table 2.

Table 2. Determination of OA in tomato and onion samples at surface of GA/GCE in 0.1 M PBS solution (pH 7.00).

Sample	Proposed method (mg/g)	Titration method (mg/g)	T_{exp}[a]	F_{exp}[b]
Tomato	4.27±0.41	3.33±0.29	2.16	1.85
Onion	6.26±0.54	5.49±0.61	3.12	3.21

[a] Experimental T test
[b] Experimental F test

The content of OA determined using the proposed sensor was 4.27 ± 0.41 mg g-1 and 6.26 ± 0.54 mg g-1 for tomato and onion, respectively. The data obtained for the analysis OA was compared favourably with that obtained by the standard method (conventional $KMnO_4$ titration). There is no significant difference between the labelled contents and those obtained by the proposed sensor. Therefore, the satisfactory results obtained with this method confirm the strong applicability of the GA/GCE in practical analysis.

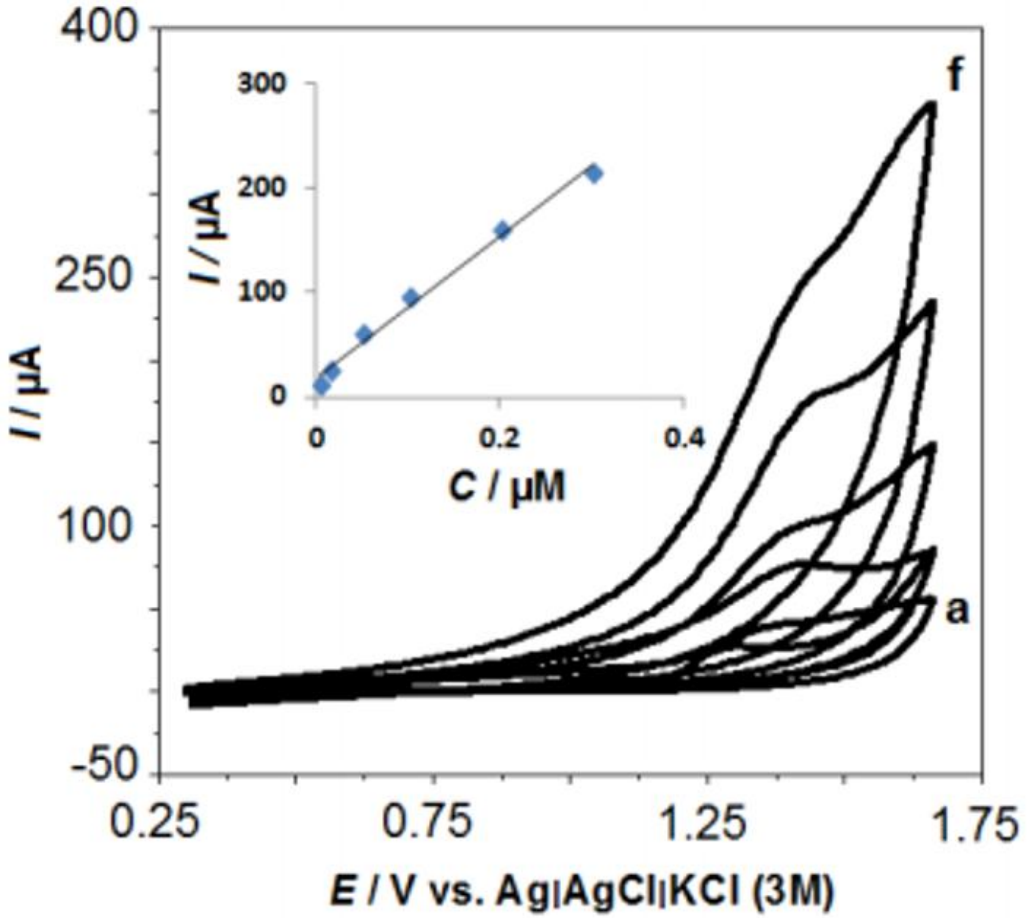

Figure 5. (A) Cyclic voltammograms of GA/GCE in the presence of (a) 4, (b) 15, (c) 50, (d) 100, (e) 200 and (f) 300 µM of OA in 0.1 M PBS solution (pH 7.00) at scan rate of 50 mV/s. (B) Plat of current vs. OA concentration.

Possible interferences for the detection of OA at the GA/CPE was tested by the addition of different compound species such as glycine, alanine, ascorbic acid, dopamine, uric acid, L-cysteine, glutathione, D-penicillamine, cystamine, N-acetyl-L-cysteine and lysine into pH 7.00 PBS in the presence of 0.05 mM OA. The results indicated that these compound species did not show clear interference.

The stability of GA/GCE was investigated every 2 days in 2 weeks. The response to 0.1 mM OA only decreased less than 14% over 2 weeks, indicating the proposed sensor has an excellent stability. In order to test the reproducibility of the proposed sensor, five individual electrodes were

fabricated and used for determining 0.05 mM OA. The results showed that the R.S.D of five lectrode is 5.2 %, indicating the proposed sensor also has an excellent reproducibility.

4. CONCLUSION

In this paper, we proposed a hydrothermal synthesis method for graphene aerogel preparation. The fabricated graphene aerogel characterized by SEM, XRD and Raman spectroscopy. The results indicate the formed graphene aerogel owing a high porous structure. Then, the prepared graphene aerosol was used for electrode surface modification and used for selective detection of OA. The proposed OA sensor shows a linear detection relationship between OA concentrations from 4 to 100 μM. Moreover, the proposed sensor exhibits a low detection limit of 0.8 μM. The sensor could sustaining stability over two weeks. We also used the proposed OA sensor for real sample detection such as tomato and onion. Therefore, our proposed OA sensor has the advantages of the operation simplicity, rapidity and low analytical cost, which could be used in filed applications.

ACKNOWLEDGEMENTS
The authors gratefully thank the Financial 423 supports from the National Natural Science Foundation of China 424 (Contract Number: 21373103)

Reference

1. A. Hodgkinson, *London—New York*, (1977)
2. G.C. Curhan, W.C. Willett, F.E. Speizer, D. SpiegelmanandM.J. Stampfer, *Annals of Internal Medicine*, 126 (1997) 497
3. A.B. IbáñezandS. Bauer, *Biotechnology for biofuels*, 7 (2014) 145
4. G. Marrubini, A. Pedrali, P. Hemström, T. Jonsson, P. AppelbladandG. Massolini, *Journal of separation science*, 36 (2013) 3493
5. A. Soleymanpour, B. Shafaatian, H.S. MirfakhraeiandA. Rezaeifard, *Talanta*, 116 (2013) 427
6. F. Chinnici, U. Spinabelli, C. RiponiandA. Amati, *Journal of food composition and analysis*, 18 (2005) 121
7. R. Hönow, D. BongartzandA. Hesse, *Clinica chimica acta*, 261 (1997) 131
8. C. Peng, H. Bai, Q. Li, Y. Guo, J. Huang, C. SuandJ. Guo, *Int. J. Electrochem. Sci*, 10 (2015) 3885
9. X. Song, H. Du, Z. Liang, Z. Zhu, D. DuanandS. Liu, *Int. J. Electrochem. Sci*, 8 (2013) 6566
10. L. Fu, Y. ZhengandA. Wang, *Int. J. Electrochem. Sci*, 10 (2015) 3518
11. Y. Zheng, L. Fu, A. WangandW. Cai, *Int. J. Electrochem. Sci*, 10 (2015) 3530
12. A. Berná, J.M. Delgado, J.M. Orts, A. RodesandJ.M. Feliu, *Langmuir*, 22 (2006) 7192
13. A. Berná, A. RodesandJ.M. Feliu, *Journal of Electroanalytical Chemistry*, 563 (2004) 49
14. H. Ahmar, A.R. Fakhari, M.R. Nabid, S.J.T. RezaeiandY. Bide, *Sensors and Actuators B: Chemical*, 171 (2012) 611
15. S. Garcia-SeguraandE. Brillas, *Water Res*, 45 (2011) 2975
16. A. Rahim, S.B. Barros, L.T. ArenasandY. Gushikem, *Electrochimica Acta*, 56 (2011) 1256
17. S.-i. Yamazaki, Y. Yamada, N. Fujiwara, T. Ioroi, Z. Siroma, H. SenohandK. Yasuda, *Journal of Electroanalytical Chemistry*, 602 (2007) 96
18. T.C. Canevari, J. Arguello, M.S. FranciscoandY. Gushikem, *Journal of Electroanalytical*

Chemistry, 609 (2007) 61
19. J. Restivo, R.P. Rocha, A.M. Silva, J.J. Órfão, M.F. PereiraandJ.L. Figueiredo, *Chinese Journal of Catalysis*, 35 (2014) 896
20. Y. Liu, J. Huang, D. Wang, H. HouandT. You, *Analytical Methods*, 2 (2010) 855
21. L. He, L. FuandY. Tang, *Catalysis Science & Technology*, 5 (2015) 1115
22. L. Fu, Y. Zheng, Z. Wang, A. Wang, B. DengandF. Peng, *Digest Journal of Nanomaterials and Biostructures*, 10 (2015) 117
23. W.S. HummersandR.E. Offeman, *Journal of the American Chemical Society*, 80 (1958) 1339
24. L. Fu, Y. Zheng, A. Wang, W. CaiandH. Lin, *Food Chemistry*, 181 (2015) 127
25. C. NethravathiandM. Rajamathi, *Carbon*, 46 (2008) 1994
26. M. Ahmad, E. Ahmed, Z.L. Hong, J.F. Xu, N.R. Khalid, A. ElhissiandW. Ahmed, *Appl Surf Sci*, 274 (2013) 273
27. X. Li, Q. Wang, Y. Zhao, W. Wu, J. ChenandH. Meng, *Journal of colloid and interface science*, 411 (2013) 69
28. D. BoukhvalovandM. Katsnelson, *Physical Review B*, 78 (2008) 085413
29. Y. Chen, X. Zhang, H. Zhang, X. Sun, D. ZhangandY. Ma, *RSC Advances*, 2 (2012) 7747
30. Y.J. Lee, G.-P. Kim, Y. Bang, J. Yi, J.G. SeoandI.K. Song, *Mater Res Bull*, 50 (2014) 240
31. F. Manea, C. Radovan, I. Corb, A. Pop, G. Burtica, P. Malchev, S. PickenandJ. Schoonman, *Sensors*, 7 (2007) 615
32. A. RezaáFakhari, *Analytical Methods*, 4 (2012) 3314
33. T.A. Ivandini, T.N. Rao, A. FujishimaandY. Einaga, *Analytical chemistry*, 78 (2006) 3467